

### III NEARBY GALAXIES OF LARGE ANGULAR SIZE

*"A difficulty in studying M31 is its rather closely edge-on view. We may take comfort from the fact that astronomers in M31 would have the same problem in studying our Galaxy"*

P.C. van der Kruit in Discussion III.6

## RADIO CONTINUUM OBSERVATIONS OF M31 AND M33

Elly M. Berkhuijsen  
Max-Planck-Institut für Radioastronomie, Bonn, F.R.G.

### 1. INTRODUCTION

The two nearest spiral galaxies, M31 and M33, have been extensively studied both at optical as well as at radio wavelengths. Reviews of radio continuum observations are given in van der Kruit and Allen (1976) and in von Kap-herr et al. (1978), respectively. In Table 1 new radio observations in various stages of progress are listed, all of which show — or are expected to show — spiral structure. In this paper the Effelsberg maps at 11 cm of M31 and at 6 cm of M33 are discussed and compared with optical data. Some attention is given to the separation of thermal and nonthermal emission which is essential to any discussion of the origin of the radiation.

### 2. M31

In Figure 1 the 11-cm map of Berkhuijsen and Wielebinski (1974) is shown superimposed onto an optical picture (Lick Observatory). Intense radio emission is seen from the nucleus and the optically bright arms, especially from arms 4 and 5 (Baade 1958). Several point sources in the radio map are coincident with known HII regions (Baade and Arp 1974), but most of the point sources are probably unrelated to M31. Berkhuijsen (1977; hereafter referred to as Paper II) subtracted the point sources from the map and made a detailed comparison of the distribution of the extended radio emission at 11 cm with the distributions of HI, HII regions, OB associations and blue light. Some conclusions of that paper are:

- (1) Apart from the nucleus the general distributions of the 11-cm continuum emission, HII regions, young stars and HI are very similar, all of them being characterised by the intense ring at about 9 kpc from the centre. This is evident from Figures 4, 5 and 6 in Paper II and can also be seen from the radial distributions shown in Figure 4 below.
- (2) The lines of maximum surface brightness in the distributions of the radio continuum, HI and HII are generally coincident with each other and often follow the dust lanes. Along the arms peaks in the

Table 1. RADIOCONTINUUM OBSERVATIONS SHOWING SPIRAL STRUCTURE

Galaxy				M31		M33		
Telescope	$\lambda$ (cm)	HPBW (')		Area (R in ')	Noise in $T_b$	Area (R in ')	Noise in $T_b$	
Cambridge	200	TP	$3 \times 5$	200	< 20 K	-	-	
	75	TP	4.0	80 <sup>a</sup>	1 K	-	-	
Westerbork	49	TP	$1.0 \times 1.5$	120 <sup>*</sup>	3	1 K	60 <sup>*</sup>	1 K
		POL	$3.6 \times 5.4$	120 <sup>b</sup>	fields	60 mK	-	-
	21	TP	$0.4 \times 0.6$	12, 20 <sup>c</sup>		1 K	-	-
	21	TP	$0.4 \times 0.6$	160	15	1 K	20 <sup>e</sup>	1 K
		POL			fields		-	-
	6	TP	$0.1 \times 0.2$	-	-	N604		
Effelsberg	21	TP	9.2	130 <sup>*</sup>	20 mK	70 <sup>*</sup>	22 mK	
		POL		130 <sup>*</sup>	11 mK	70 <sup>*</sup>	12 mK	
	11	TP	4.8/4.5	125, 105 <sup>d</sup>	4.5 mK	60 <sup>*</sup>	4 mK	
		POL		90	2.5 mK			
	6	TP	2.6	20 <sup>*</sup>	2.3 mK	45 <sup>f</sup>	2.3 mK	
	TP		90					

a) Pooley 1969; b) Segalovitz et al. 1977; c) van der Kruit 1972;  
d) Berkhuijsen, Wielebinski 1974; e) Israel, van der Kruit 1974;  
f) von Kap-herr et al. 1978; \* observed and partly reduced;  
rest: accepted proposals, partly observed  
Area: determined by  $R$  = distance from center along major axis.

continuum emission are typically 2 kpc apart; they are usually found near to but not coincident with peaks in the distributions of HI or HII. These properties are in agreement with the predictions of Mouschovias et al. (1974).

(3) The large-scale correlations between the various constituents can be described by power laws. For example it was found that the number of HII regions in the radio beam  $N_{\text{HII}} \propto T_b^{2.9}$  ( $T_b$  = observed brightness temperature due to thermal + nonthermal emission along the line of sight in M31). Recent independent measurements at 11 cm (Beck, Berkhuijsen, Wielebinski), however, suggest a different zerolevel for the 11-cm map than has been assumed in Paper II; this may change the power law to  $N_{\text{HII}} \propto T_b^{2.0}$ . If  $N_{\text{HII}}$  is proportional to the total thermal emission (i.e. including diffuse emission and undetected HII regions) then a power law with an exponent  $> 1$  indicates that the nonthermal radiation is more smoothly distributed than the thermal radiation. A steepening of the spectrum with increasing distance from the center is then to be expected.

A first attempt to find the spectral index distribution across M31 is being made by Beck et al. (1978). Comparison of the 21-cm map recently observed in Effelsberg with the 11-cm map smoothed to the

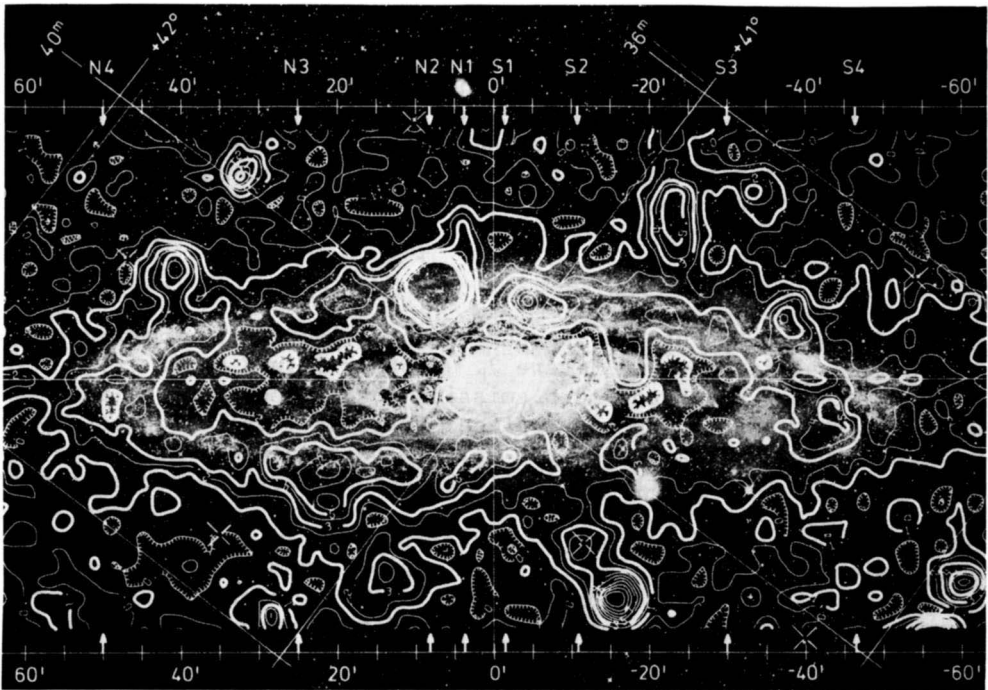


Fig. 1. Contour map of M31 at 11 cm including unrelated point sources (contour interval = 15 mK in  $T_b$ ) superposed onto a Lick photograph. The scale along the minor axis is the same as that along the major axis.

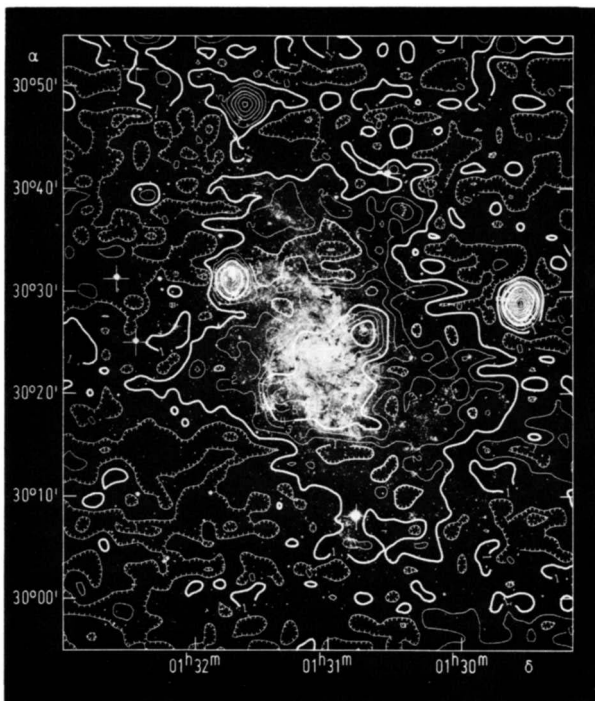


Fig. 2. Contour map of M33 at 6 cm superposed onto a Lick picture (contour interval = 8 mK in  $T_b$ ). A plus indicates the position of the optical center (von Kap-herr et al. 1978).

beamwidth at 21 cm does indeed show a steepening of the spectrum towards the outer regions of M31. The preliminary results indicate a striking difference between the northern and the southern half of M31: in the north the spectrum is nearly constant, while in the south it steepens strongly towards the outer regions. We are presently investigating whether this difference might be related to asymmetries between north and south in other constituents that are known to exist in M31 (Paper II).

### 3. M33

The 6-cm map of M33 of von Kap-herr et al. (1978) superimposed onto a Lick photograph is shown in Figure 2. Contour 1 (= 8 mK in  $T_b$ ) encloses an area of extended radio emission roughly centered on the galaxy and partly coinciding with optical features. The strongest emission inside contour 1 comes from the HII region complexes NGC 604 and NGC 595, and from some of the optically brightest parts near the center.

The catalogue of HII regions in M33 of Boulesteix et al. (1974) gives emission measure and size for each region, from which the expected flux at 6 cm can be derived. The total flux of these optically detected regions appears to contribute 26% of the integrated flux at 6 cm within 40' from the center in the plane of M33. The observed diffuse emission of emission measure  $E \approx 50 \text{ cm}^{-6} \text{ pc}$  within 20' from the center (Boulesteix, Laval 1975) adds 32% of thermal radiation. Hence, within 40' from the center the thermal fraction of the integrated flux at 6 cm is  $\approx 0.58$ ; this is a lower limit since absorption effects, missed HII regions and diffuse emission weaker than observed are not taken into account.

The thermal fraction as a function of distance to the center  $f_{th}(R)$  was studied by comparing the expected thermal emission in the Effelsberg beam at 6 cm with the observed radio emission, both averaged in rings of 2' width around the center. It was assumed that the thermal fraction at the center  $\leq 1.0$ , and that the total thermal emission has the same radial distribution as the detected HII regions. Figure 3a shows that  $f_{th}(R)$  generally decreases with increasing  $R$ . In this case  $f_{th}(R < 40') = 0.68$  for the integrated flux, only slightly larger than the lower limit of 0.58, suggesting that absorption and other effects are not very large. With  $f_{th}(R < 40') = 0.68$  and a spectral index of the integrated emission  $\alpha = 0.52$  (von Kap-herr et al. 1978) the spectral index of the nonthermal emission  $\alpha_n = 0.85$  is found. If  $\alpha_n$  is constant for  $R < 40'$  the expected variation of the total spectral index  $\alpha(R)$  can be derived from  $f_{th}(R)$  (Figure 3a); we eventually hope to check  $\alpha(R)$  by comparing with observations at other frequencies.

Knowing  $f_{th}(R)$  the thermal emission  $T_{th}$  and nonthermal emission  $T_n$  can be separated (Figure 3b). The radial distribution of  $T_n$  is significantly flatter than that of  $T_{th}$ ; this suggests that either the objects X that produce the relativistic electrons have a distribution quite different from that of the HII regions or, if the objects X are

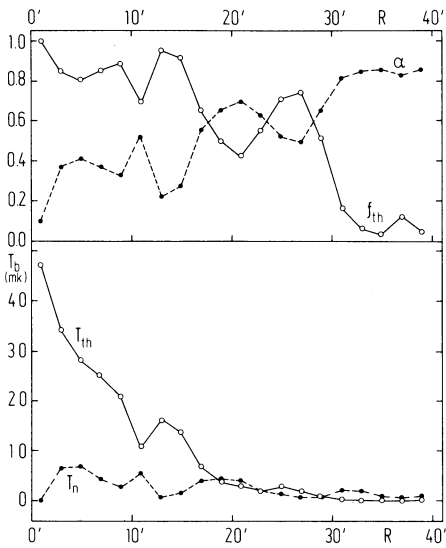


Fig. 3. Radial distribution in M33 of a (top): thermal fraction  $f_{th}$  and expected total spectral index  $\alpha$ ; b (bottom): thermal emission  $T_{th}$  and non-thermal emission  $T_n$ .

distributed like the HII regions, strong diffusion of relativistic electrons in the disk outwards is taking place. A similar conclusion was reached by van der Kruit (this volume) for M51.

4. RADIAL DISTRIBUTIONS

The radial distributions of various constituents in M31 and M33 are shown in Figures 4 and 5, respectively. M31 is an Sb-galaxy with both a significant nuclear bulge as well as a disk component. Both components are visible in the curves of the radio continuum, blue light and total mass. The disk component has its maximum at the bright ring at  $R \approx 9$  kpc as is evident from the curves of HII regions, OB associations and HI. The surface brightness (or surface density, depending on which constituent is considered) of the disk component decreases exponentially from  $R \approx 9$  kpc outwards (see Paper II for details).

M33 is of Hubble type Sbc and consists mainly of a disk component which has its maximum near the center. For  $R=0$  to  $R \approx 7$  kpc the surface brightness or surface density of total mass, blue light, radio continuum and HII regions decreases exponentially, while that of HI remains constant. Beyond  $R \approx 7$  kpc the surface density of HI and of HII regions drops suddenly. For comparison a distribution of supernovae is shown. Note, however, that this curve does not represent the specific distribution of SN in M31 or M33, but a sum distribution of some 150 galaxies; the 2 values closest to the center are unreliable.

If the surface brightness or surface density decreases as  $\sigma(R) = \sigma(0) e^{-R/L}$  the scale length  $L$  normalised with the Holmberg radius,  $L/R_{Ho}$ , can be derived for the disk component. In both galaxies the exponential part of the disk component (i.e.  $8 < R \lesssim 20$  kpc in M31, and  $0 < R < 7$  kpc in M33) in blue light yields  $L/R_{Ho} = 0.25 \pm 0.01$ . To within the errors the other constituents have this same scale length apart from HI in M33, and the HII regions ( $0.13 \pm 0.01$ ) and OB associations ( $0.17 \pm 0.01$ ) in M31. These observations may be a challenge to galaxy-model makers.

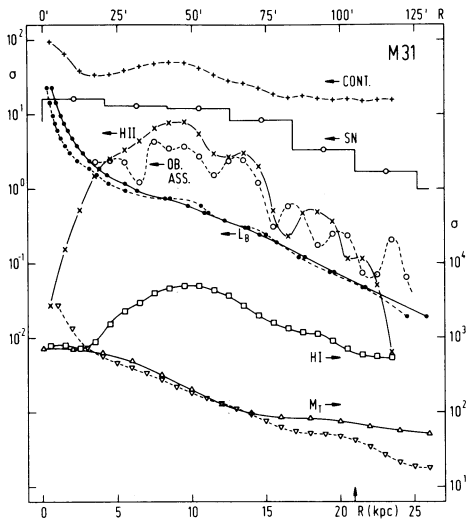


Fig. 4. Radial distribution of various constituents in M31: CONT - 11-cm radio continuum (Berkhuijsen 1977), SN - supernovae (Iye, Kodaira 1975), HII - HII regions (Baade, Arp 1964), OB.ASS. - OB associations (van den Bergh 1964; Richter 1971),  $L_B$  - blue light (de Vaucouleurs 1958), HI - neutral hydrogen (Emerson 1974),  $M_T$  - total mass ( $\Delta$  Roberts, Whitehurst 1975;  $\nabla$  Emerson 1976).

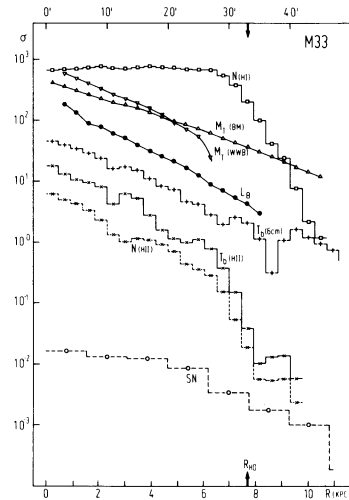


Fig. 5. Radial distribution of various constituents in M33: N(HI) - neutral hydrogen (Rogstad et al. 1976),  $M_T$  - total mass ( $\Delta$  Boulesteix, Monnet 1970;  $\nabla$  Warner et al. 1973),  $L_B$  - blue light (de Vaucouleurs 1959),  $T_6$  (6 cm) - 6-cm radio continuum (von Kap-herr et al. 1978),  $T_B$  (HII) and N(HII) - brightness temperature and surface density of individual HII regions only (Boulesteix et al. 1974), SN - supernovae (Iye, Kodaira 1975).

## 5. CONCLUSIONS

Both in M31 as well as in M33 a large-scale similarity in the distribution of the various constituents appears to exist. In both galaxies the surface brightness of the disk component decreases exponentially from its maximum outwards; the normalised scale length of blue light and of several other constituents is 0.25.

The origin of the radio continuum radiation is still unclear. In M33 at least 60% of the integrated flux for  $R < 40'$  is thermal. The radial distribution of the nonthermal emission is much flatter than that of the thermal emission and of supernovae suggesting that supernovae are not the only sources of relativistic electrons. In M31 the situation is similar. The minimum in the radial distribution of the continuum radiation at  $R \approx 4$  kpc in this galaxy indicates that diffusion of relativistic electrons from the nucleus into the spiral arms cannot

significantly contribute to the emission from the arms.

Finally: much remains to be observed! For instance, in the radio continuum the distribution of polarised radiation at various wavelengths could tell us more about the nonthermal radiation and magnetic fields; the distribution of the thermal emission could be derived from observations at  $\lambda \approx 2$  cm. Combination of the latter data with the distributions of the total flux (i.e. integrated along the line of sight) in H $\alpha$  and/or H $\beta$  would give information on the distribution of diffuse HII emission and of optical absorption; data on the distribution of young stars and of the surface brightness in blue light (and other colours) could be improved; the distribution of optical polarisation is still unknown. The proximity to M31 and M33 makes these observations — although time consuming — extremely interesting.

#### REFERENCES

- Baade, W.: 1958, *Ric. Astron. Specula. Astron. Vatic.* 5, 1.  
 Baade, W., Arp, H.C.: 1964, *Astrophys. J.* 139, 1027.  
 Beck, R., Berkhuijsen, E.M., Baker, J.R., Wielebinski, R.: 1978, in preparation.  
 Bergh, S. van den: 1964, *Astrophys. J. Suppl. Series* 86, 65.  
 Berkhuijsen, E.M.: 1977, *Astron. Astrophys.* 57, 9.  
 Berkhuijsen, E.M., Wielebinski, R.: 1974, *Astron. Astrophys.* 34, 173.  
 Boulesteix, J., Courtès, G., Laval, A., Monnet, G., Petit, H.: 1974, *Astron. Astrophys.* 37, 33.  
 Boulesteix, J., Laval, A.: 1975, private communication.  
 Boulesteix, J., Monnet, G.: 1970, *Astron. Astrophys.* 9, 350.  
 Emerson, D.T.: 1974, *Monthly Notices Roy. Astron. Soc.* 169, 607.  
 Emerson, D.T.: 1976, *Monthly Notices Roy. Astron. Soc.* 176, 321.  
 Israel, F., Kruit, P.C. van der: 1974, *Astron. Astrophys.* 32, 363.  
 Iye, M., Kodaira, K.: 1975, *Publ. Astron. Soc. Japan* 27, 411.  
 Kap-herr, A. von, Berkhuijsen, E.M., Wielebinski, R.: 1978, *Astron. Astrophys.* 62, 51.  
 Kruit, P.C., van der, Allen, R.J.: 1976, *Ann. Rev. Astron. Astrophys.*, p. 417.  
 Mouschovias, T.Ch., Shu, F.H., Woodward, P.R.: 1974, *Astron. Astrophys.* 33, 73.  
 Richter, G.A.: 1971, *Astron. Nachr.* 292, 275.  
 Roberts, M.S., Whitehurst, R.N.: 1975, *Astrophys. J.* 201, 327.  
 Rogstad, D.H., Wright, M.C.H., Lockhart, I.A.: 1976, *Astrophys. J.* 204, 703.  
 Vaucouleurs, G. de: 1958, *Astrophys. J.* 128, 465.  
 Vaucouleurs, G. de: 1959, *Astrophys. J.* 130, 728.  
 Warner, P.J., Wright, M.C.H., Baldwin, J.E.: 1973, *Monthly Notices Roy. Astron. Soc.* 163, 163.

#### DISCUSSION FOLLOWING PAPER III.1 GIVEN BY E.M. BERKHUIJSEN

VAN DER KRUIT: How sensitive is your estimate that in M33 about 60% of



the flux density at 6.2 cm is thermal to an assumed optical absorption in the foreground, to absorption internal to the HII regions and to variations of absorption across the disk?

BERKHUIJSEN: Optical absorption did not enter my estimate. I find that 58% of the integrated flux density of M33 is thermal by just adding the flux densities of the optically detected HII regions and of the detected diffuse emission. So 58% is a lower limit. However, this lower limit does also depend on the total integrated flux density of M33 which is uncertain by a factor of 0.2. Therefore the lower limit for the thermal fraction is  $0.58 \pm 0.12$ .

VAN WOERDEN: How many hours of observation are required to map M31 at 6 cm?

BERKHUIJSEN: With the present system about 200 hours under perfect weather conditions.

BURKE: How complete is the correspondence between the radio maxima of the smooth component at 11 cm and the optically dark regions in M31? Is the correspondence significant or chance?

BERKHUIJSEN: There is not a one-to-one correspondence but I don't think it is chance. On the edges of the dust lanes most of the HII regions are found, and I have derived an empirical relation for the number of HII regions in the radio beam and the brightness temperature at 11 cm. This relation takes the form  $N_{\text{HII}} \propto T_{\text{b}}^{2.9 \pm 0.6}$ . Furthermore, the peak lines in the HI distribution derived by Emerson, with an angular resolution of about 2', closely follow the dust lanes. After smoothing of his HI distribution to the 11-cm beamwidth of 4'.8, in the bright ring the HI peak lines coincide very well with the peak lines in the distribution of the emission at 11 cm [see also Bystedt's comment below].

BECK: VARIATION OF SPECTRAL INDEX ACROSS M31

Using the 11-cm map of Berkhuijsen and Wielebinski (1974, A.A. 34, 173) and our new 21-cm map (Beck, Berkhuijsen, Baker, Wielebinski) I have calculated the distribution of the spectral index across M31 after subtraction of point sources and careful correction of the baselevels of the maps. There is a large-scale asymmetry between the northern and the southern half of M31 out to 15 kpc from the center. The average temperature spectral index  $\beta$  in the north is  $0.36 \pm 0.05$  lower than in the south ( $T_{\text{b}} \propto \nu^{-\beta}$ ). Baseline errors cannot explain this effect. From data averaged in rings an increase of the spectral index with radius is evident in the southern half of M31, but the spectral index is constant within the errors in the northern half.

BALDWIN: How large were the spectral variations in M31 before making serious corrections to the baselevel, i.e. we need to know how serious is serious.

BECK: Before corrections to the baselevels were made the spectral variations were even larger than I have shown.

BERKHUIJSEN: In other words: we cannot explain the steepening of the spectrum with the errors we can think of.

DAVIES: Can the difference in spectral index between the north and south of M31 be explained quantitatively by the known asymmetry of HII regions?

BERKHUIJSEN: For M31 we only know the number - density distribution of HII regions, not the distribution of emission in H $\alpha$ . Therefore, we cannot yet calculate the variation of the thermal fraction across the disk which is the relevant parameter that influences the spectral index.

VAN DER KRUIT: It must be realized that M31 and M33 have weak disks in the radio emission compared to other galaxies; thermal emission is definitely going to have a very strong effect.

BYSTEDT: M31 AT 49 CM WAVELENGTH

Observations at 610 MHz with the Westerbork telescope (Israel, de Bruyn and Bystedt) of M31 clearly show the bright continuum ring associated with the strongest optical arm. There is a strong asymmetry between the NW arm which is narrow and closely follows a dust lane, and the SE arm which is much broader and not clearly related to any detailed optical features. The highest peaks in both arms are of about the same strength.

There also seems to be emission extending from the nuclear region to the ring approximately in the minor axis direction.

ALLEN: Can you be sure that the connection between the arms and the nucleus in the radio maps is not merely a projection effect?

BYSTEDT: In no other place do we see emission inside the dark ring, but a projection effect cannot be ruled out.